HAL
open science

SUGT1 controls susceptibility to HIV-1 infection by stabilizing microtubule plus-ends

Awatef Allouch, Cristina Di Primio, Audrey Paoletti, Gabrielle Lê-Bury, Frédéric Subra, Valentina Quercioli, Roberta Nardacci, Annie David, Héla Saidi, Anna Cereseto, et al.

To cite this version:

Awatef Allouch, Cristina Di Primio, Audrey Paoletti, Gabrielle Lê-Bury, Frédéric Subra, et al.. SUGT1 controls susceptibility to HIV-1 infection by stabilizing microtubule plus-ends. Cell Death and Differentiation, 2020, Online ahead of print, pp.18 - 22. 10.1038/s41418-020-0573-5 . pasteur-02868173

HAL Id: pasteur-02868173

https://pasteur.hal.science/pasteur-02868173v1

Submitted on 18 Jun 2020

HAL is a multi-disciplinary open access archive for the deposit and dissemination of scientific research documents, whether they are published or not. The documents may come from teaching and research institutions in France or abroad, or from public or private research centers.

L'archive ouverte pluridisciplinaire **HAL**, est destinée au dépôt et à la diffusion de documents scientifiques de niveau recherche, publiés ou non, émanant des établissements d'enseignement et de recherche français ou étrangers, des laboratoires publics ou privés.

SUGT1 controls susceptibility to HIV-1 infection by stabilizing microtubule plus-ends

Awatef Allouch[1-4], Cristina Di Primio[5], Audrey Paoletti[1-4], Gabrielle Lê-Bury[6-8], Frédéric Subra[9], Valentina Quercioli[5], Roberta Nardacci[10], Annie David[11], Hela Saidi[12], Anna Cereseto[13], David M. Ojcius[14,15], Guillaume Montagnac[16], Florence Niedergang[6-8], Gianfranco Pancino[11], Asier Saez-Cirion[11], Mauro Piacentini[10,17], Marie-Lise Gougeon[12], Guido Kroemer[8,18-22] and Jean-Luc Perfettini[1-4,14]

[1] Cell death and Aging team, Gustave Roussy Cancer Campus, F-94805 Villejuif, France;
[2] Laboratory of Molecular Radiotherapy, INSERM U1030, Gustave Roussy Cancer Campus, F-94805 Villejuif, France;
[3] Gustave Roussy Cancer Campus, F-94805 Villejuif, France;
[4] Université Paris Sud Saclay, 114 rue Edouard Vaillant, F-94805 Villejuif, France;
[5] Bio@SNS Laboratory, Scuola Normale Superiore, Piazza dei Cavalieri 7, 56126 Pisa, Italy;
[6] INSERM U1016, Institut Cochin, F- 75013 Paris, France;
[7] CNRS, UMR 8104, F- 75013 Paris, France;
[8] Université Paris Descartes, Université de Paris, F-75006 Paris, France;
[9] CNRS UMR 8113 LBPA, Ecole Normale Supérieure de Cachan, 61 avenue du Président Wilson, F-94230 Cachan, France;
[10] National Institute for Infectious Diseases "Lazzaro Spallanzani", Via Portuense 292, I-00149 Rome, Italy;
[11] Unité HIV inflammation and Persistance, 28 rue du Dr Roux, F-75015 Paris, France;
[12] Antiviral Immunity, Biotherapy and Vaccine Unit, Institut Pasteur 25 rue du Dr. Roux, F-75015 Paris, France;
[13] Laboratory of Molecular Virology, University of Trento, Centre for Integrative Biology, Via Sommarive 9, I-38123 Povo (Trento), Italy;
[14] Department of Biomedical Sciences, University of the Pacific, Arthur Dugoni School of Dentistry, San Francisco, CA 94103;
[15] Université de Paris, F-75013 Paris France;
[16] INSERM U1170, Gustave Roussy Cancer Campus, F-94805 Villejuif, France;
[17] Department of Biology, University of Rome "Tor Vergata", Via della Ricerca Scientifica 1, I-00173, Rome, Italy;
[18] INSERM U848, Gustave Roussy Cancer Campus, F-94805 Villejuif, France;
[19] Metabolomics Platform, Gustave Roussy Cancer Campus, F-94805 Villejuif, France;
[20] Equipe 11 labellisée Ligue contre le Cancer, Centre de Recherche des Cordeliers, INSERM U1138, F-75006 Paris, France;
[21] Pôle de Biologie, Hôpital Européen Georges Pompidou, AP-HP, F-75015 Paris, France;
[22] Karolinska Institute, Department of Women's and Children's Health, Karolinska University Hospital, S-17176 Stockholm, Sweden.

The authors declare they have no conflicts of interest

Running title: SUGT1 stabilizes microtubules for HIV-1 infection

Keywords: HIV-1; microtubules; nuclear import; SUGT1

Corresponding author:
Dr. Jean-Luc PERFETTINI
Cell death and Aging team
Laboratory of Molecular Radiotherapy, INSERM U1030
Gustave Roussy Cancer Campus
F-94805 Villejuif, France
Tel. 33-1-42 11 54 24
Fax 33-1-42 11 66 65
e-mail: perfettini@orange.fr
ORCIDid: https://orcid.org/0000-0002-2427-2604

Abstract

Understanding the viral-host cell interface during HIV-1 infection is a prerequisite for the development of innovative antiviral therapies. Here we show that the suppressor of G2 allele of *skp1* (SUGT1) is a permissive factor for human immunodeficiency virus (HIV)-1 infection. Expression of SUGT1 increases in infected cells on human brain sections and in permissive host cells. We found that SUGT1 determines the permissiveness to infection of lymphocytes and macrophages by modulating the nuclear import of the viral genome. More importantly, SUGT1 stabilizes the microtubule plus-ends (+MTs) of host cells (through the modulation of microtubule acetylation and the formation of end-binding protein 1 (EB1) comets). This effect on microtubules favors HIV-1 retrograde trafficking and replication. SUGT1 depletion impairs the replication of HIV-1 patient primary isolates and mutant virus that is resistant to raltegravir antiretroviral agent. Altogether our results identify SUGT1 as a cellular factor involved in the post-entry steps of HIV-1 infection that may be targeted for new therapeutic approaches.

Introduction

The design of novel therapeutic antiviral approaches to inhibit the replication of drug-resistant HIV-1 strains assumes a detailed understanding of the cellular factors that promote viral replication steps. Independently from the process of viral entry into target cells, HIV-1 rapidly traffics on stable microtubules, which are characterized by high acetylation levels of α-tubulin at lysine 40 (K40), to reach the nucleus and integrate in the human genome (1, 2). A large list of microtubule-binding proteins is involved in HIV-1 uncoating and stabilization of viral complexes to accomplish reverse transcription and cytoplasmic viral trafficking (reviewed in (3)). Since the suppressor of G2 allele of *S phase kinase associated protein-1 (skp1)* (SUGT1) protein can attach proteins onto microtubules (4-8), we investigated the role of SUGT1 in the early cellular response to HIV-1 infection. Initially described as a co-chaperone of heat shock protein 90, SUGT1 is involved in the innate immune response in plants and mammals (9) through the activation of nucleotide binding domain and leucine-rich repeat containing (NLRP) proteins. Here, we showed that SUGT1 is a permissive cellular factor for HIV-1 infection. We demonstrated that SUGT1 promotes HIV-1 reverse transcription and nuclear import through the stabilization of microtubule plus-ends that are required for efficient HIV-1 cytoplasmic trafficking. Altogether, our results identify and characterize SUGT1 as a cellular factor that is essential for early steps of HIV-1 infection.

Materials and Methods

Cells and reagents

Buffy coats from healthy donors were obtained through the French blood bank (Etablissement Français du sang (EFS)) as part of EFS-INSERM Convention in accordance with French law. Monocytes were obtained from buffy coats and differentiated into macrophages as previously described (10). Monocytes were first separated from peripheral blood mononuclear cells (PBMCs) by adherence to the plastic and then cultured for 6 to 7 days in hydrophobic Teflon dishes (Lumox; Duthsher) in macrophages medium (RPMI 1640 supplemented with 200 mM L-glutamine, 100 U of penicillin, 100 µg streptomycin, 10 mM HEPES, 10 mM sodium pyruvate, 50 µM β-mercaptoethanol, 1% minimum essential medium vitamins, 1% non-essential amino acids) containing 15% of heat inactivated human serum AB. MDMs were then harvested and suspended in macrophage medium containing 10% of heat inactivated fetal bovine serum (FBS). Flow cytometry analysis using anti-CD14 (eBioscience, #12-0149-42), anti-CD11b (Pharmingen, #557918), anti-CD71 (Pharmingen, #555537), anti-CD163 (Pharmingen, #562669), anti-CD206 (Pharmingen, #551135) antibodies revealed that 91 to 96 % of MDMs expressed both differentiation (CD14, CD11b and CD71) and M2 macrophage (CD163 and CD206) markers. The purity of MDMs was also controlled by the negative staining for anti-CD56 (#560916) (NK cells), anti-CD3 (#555339) (T cells) and anti-CD20 (#559776) (B cells) antibodies. All antibodies used were from Pharmingen. The PBLs were isolated from the non-adherent PBMCs fraction using T cells negative selection kit (STEM CELL). Lymphocytes obtained by this method were 90 to 97% CD3 expressing T cells and were cultured in RPMI medium containing 10% FBS. T lymphocytes ($5x10^6$/ml) were stimulated by phytohemagglutinin (PHA-P) (5 µg/ml) for 72 hours in medium containing IL-2 (25 units/ml) (Roche), suspended at 10^6/ml in IL2 medium and cultured for additional two

days for Western blot (WB) analysis of SUGT1 expression level and HIV-1 infection, and three days for SUGT1 mediated siRNA silencing. Activation of T cells was determined with anti-CD25 (BD Pharmigen, #560987) and anti-CD69 (BD Pharmigen, #557049) antibodies by flow cytometry. HeLa $CD4^{+}CXCR4^{+}$, HEK293T cells and U2OS cell lines were obtained from Prof. Guido Kroemer (Gustave Roussy Cancer Campus, France) and HeLa cells were obtained from Dr. Guillaume Montagnac (Gustave Roussy Cancer Campus, France). These cell lines were cultured in Dulbecco's modified Eagle's medium (DMEM)-Glutamax supplemented with 10% FBS and 100 UI/ml penicillin-streptomycin. All cell lines used were mycoplasma-free.

Human autopsies

Human autopsies from frontal cortex were obtained in accordance with Italian and EU legislations, after approval by the Institutional Review Board of the Italian Lazzaro Spallanzani National Institute for Infectious Disease (Ethics Committee approval number 40/2006). Post-mortem frontal cortex sections were obtained from three uninfected individuals and nine individuals with HIV-1-associated dementia (all men, mean age 36 years; the median values of HIV-1 viral load was 4.5±0.6 $\log_{10}$ cp/ml and <500 CD4 T cells/ml). All individuals consented to the research use of their frontal cortex brain autopsies at post-mortem.

RNA interference

The siGenome smart small interfering RNAs (siRNAs) were all purchased from Dharmacon. The siRNA against SUGT1 (siSUGT1) gene is composed a pool of four siRNAs. The indicated siRNAs have the following sequences: siSUGT1: (1) 5'-GAUCAAGAAUGUUCAGAAG-3', (2) 5'-GAACUUCUUCAUCCUAUAA-3', (3) 5'-

146 GCAAAGAAGUCUCUAGAAC-3' and (4) 5'- GAACCUAUAUCCAUCAUCA-3'. The
147 control siRNA is a pool of four on target plus non-targeting siRNAs (siCo.). The single
148 siRNA against SUGT1 (siSUGT1-1) used for HeLa $CD4^+CXCR4^+$ cell lines was previously
149 described (9): 5'AAGGCUUUGGAACAGAAACCA-3' and the corresponding control
150 siRNA: 5'-UUCAAUAAAUUCUUGAGGU-3' were both synthetized from Sigma.
151 Macrophage silencing was previously described with some modifications (10). Briefly,
152 MDMs ($1x10^6$/ml of macrophages medium + 10% FBS) were allowed to be attached at 37°C
153 for 2 hours prior to siRNAs transfection, which was performed with the INTERFERin
154 (Polyplus Transfection). siSUGT1 or siCo. (8 µl from 20 µM stock solution) were pre-diluted
155 in 1 ml of Opti-MEM in which 40 µl of INTERFERin were added and the transfection mix
156 was incubated at room temperature for 10 minutes. The transfection mix (500 µl) was added
157 to 10^6 for 50 nM final siRNA concentration. MDMs were then incubated at 37°C for 24 hours
158 and the medium was replaced with fresh macrophage medium supplemented with 10% FBS
159 for additional 48 hours prior infections. Activated lymphocytes were suspended in RPMI-IL2
160 medium (10^7 PBLs/ml) to which 125 µl of the transfection mix containing: 1 ml Opti-MEM,
161 20 µl INTERFERin and 4 µl of siRNA from 20 µM stock solution were added for 6.25 nM
162 final siRNA concentration. After six hours incubation, PBLs were suspend in fresh RPMI-IL2
163 medium (5 10^6 cells/ml) and cultured for additional 72 hours prior HIV-1 infection. For
164 HeLa, HEK293T and U2OS cells, the final siRNAs concentrations were at 10 picomol
165 transfected with RNAi MAX (Promega) following the manufacturer's instructions. Cell
166 lysates were assayed for protein expression by Western blot to determine the knockdown
167 efficiency at infection at 72 hours for MDMs, PBLs and HEK293T cells and 48 hours for
168 U2OS and HeLa cells post-silencing. Cell viability and cytotoxicity following silencing were
169 determined by WST-1 assay, MTT assay or the lactate dehydrogenase (LDH) release assay
170 (all from Sigma).

Plasmid transfections

HEK293T cells (2.5 10^6) were transfected with 5 µg pcDNA3-HA-IN (HA-IN) pcDNA3-HA (HA) empty vector using Fugene (Promega). After 48 hours of transfection, cells were harvested for co-immunoprecipitation assays. U2OS cells (5 10^3) were silenced by siSUGT1 (20 nM) and siControl siRNAs using RNAi max (Qiagen) and at 24 hours later were transfected with 0.5 µg pcDNA3-HA-IN or pcDNA3-HA for 24 hours. For bulk SUGT1 overexpression, HEK293T cells (10^5) were transfected with 0.75 µg of pCMV-SPORT6-SUGT1 (SUGT1) or pEGFP-N1-GFP control plasmid using Fugene (Promega). After 48 hours of transfection, cells were infected and analysed by western blots. For GFP-based flow cytometry sorting, HEK293T cells (10^5) were transfected with 0.75 µg of pRLL-EF1-SUGT1-PGK-GFP using Fugene (Promega). After 48 hours of transfection, the GFP^- and GFP^+ cells were sorted by FACS, kept for further 24 hours prior western blot analysis and infections.

Viral constructs, viruses, lentiviral vectors and in vitro infections and transductions

Single round HIV-1 infections were performed with the VSV-G envelop pseudotyped viruses: HIV-$1_{\Delta EnvNL4-3-Luc}$ and HIV-$1_{\Delta EnvNL4-3-IND64E}$ that contain luciferase as a reporter gene, HIV-$1_{\Delta EnvNL4-3-GFP-Vpr}$ that incorporates GFP-Vpr molecules or with HIV-1CMV-GFP-I-SCEI. HIV-$1_{\Delta EnvNL4-3-Luc}$, HIV-$1_{\Delta envNL4-3-IND64E}$ and HIV-$1_{\Delta EnvNL4-3-GFP}$ were obtained through the co-transfection of 3 10^6 HEK293T cells with 20 µg pNL4.3-Luc Nef- Env-, pD64E, both from NIH AIDS research reagents and 5 µg pMD2-VSV-G expression vectors following calcium phosphate transfection procedure (Promega). HIV-$1_{\Delta EnvNL4-3-GFP-Vpr}$ was obtained through the transfection of 3 10^6 HEK293T cells with 10 µg pNL4-3-Luc Nef- Env- (NIH AIDS research reagents), 2.5 µg pGFP-Vpr and 2.5 µg pMD2-VSV-G expression vectors using Fugene (Promega) following manufacturer's instructions. For HIV-$1_{\Delta EnvNL4-3-GFP-Vpr}$ (VSV-G)

196 supernatants harvest at 48 hours post-transfection and were concentrated by 2 hours of
197 ultracentrifugation in 20% (wt/vol) sucrose cushion. VSVG-pseudotyped HIV-$1_{CMV-GFP-I-SCEI}$
198 was obtained as previously described (11). Briefly, HIV-$1_{CMV-GFP-I-SCEI}$ virions were produced
199 by transient transfection of 3 10^6 HEK293T cells by using 150 nM polyethylenimine (PEI)
200 reagent (Sigma) with 20 µg of pHR-CMVGFP-I-SceI plasmid, 15 µg of pΔ8.91 packaging
201 and 5 µg of pVSV-G envelope expressing plasmid. Supernatants were collected after 48
202 hours, filtered through a 0.45 µm pore size filter and then concentrated by ultracentrifugation
203 in 20% (wt/vol) sucrose cushion. HIV-$1_{IN-EGFP}$ virions (12) were produced by transfecting 3
204 10^6 HEK293T cells by using 150 nM polyethylenimine (PEI) reagent (Sigma) with 6 µg of
205 pVpr-IN-EGFP, 6 µg of pD64E and 1 µg of pVSV-G. Supernatants were collected after 48
206 hours, filtered through a 0.45 µm pore size filter and then concentrated by ultracentrifugation.
207 For replication competent viruses HIV-1_{NL4-3} and HIV-1_{AD8} were obtained through the
208 transfection of 3 10^6 HEK293T cells with 15 µg of pHIV-1-NL4-3 and pHIV-1-AD8
209 following calcium phosphate transfection protocol (Promega). HIV-$1_{NL4-3-IN140/148}$ replication
210 competent virus (13) was pseudotyped with VSV-G to allow its entry in macrophages. Viral
211 particles in the cell supernatant were harvested at 48 hours post transfection, passed through
212 0.45 µm pore size filters and viral titers were determined by p24 content quantification by
213 ELISA (PerkinElmer).
214 MDMs and PBLs (10^6) were infected with 100 ng p24 of HIV-1_{AD8}, HIV-1_{NL4-3}, HIV-$1_{132w,}$
215 HIV-1_{BXO8} , HIV-1_{DH12} or the VSV-G envelope pseudotyped viruses (HIV-$1_{\Delta EnvNL4-3-Luc}$,
216 HIV-$1_{\Delta EnvNL4-3-IND64E}$ or HIV-$1_{\Delta EnvNL4-3-IN140/148}$) for four hours at 37°C. For HIV-1 long
217 replication, MDMs or PBLs (10^6) were infected with 400 ng CAp24 of HIV-1_{AD8} or 200 ng
218 CAp24 HIV-1_{NL4-3}, respectively. Every three days, cell supernatants were harvested and
219 replaced with fresh culture medium (10^6 MDMs/ml and 2 10^6 PBLs/ml) during 21 days. Viral
220 replication was monitored by quantifying CAp24 release in the cell supernatants using ELISA

221 method (PerkinElmer). For viral cDNA detection with qPCR, the viral stocks were pretreated
222 with benzonase (Sigma) for 20 minutes at room temperature. The infections were determined
223 by p24 content quantification by ELISA (Zeptometrix Crop) in the supernatant of cells, the
224 luciferase activity from HIV-$1_{\Delta EnvNL4-3-Luc}$ (VSV-G) in lysed cells using Luciferase kit
225 (Promega) and also by qPCR analysis of HIV-1 cDNA species at different time points. For
226 HIV-$1_{CMV-GFP-I-SCEI}$ (VSV-G) infection, HEK293T cells lines (0.5 10^5) were transfected with
227 siSUGT1 or siCo siRNAs at 10 picomol in 500 µl complete medium using RNAi max
228 (Qiagen). At 72 hours post silencing, 1 µg of pCBASce plasmid encoding ISCeI endonuclease
229 were transfected using Fugene (Promega). Six hours post-transfection cells (0.2 10^6) were
230 infected using 600 ng p24 of the virus for two hours at 37°C and then fresh medium was
231 replaced and cells were cultured for further 48 hours, detached and let to adhere on poly-L-
232 lysine solution (Sigma) pretreated chamber slides for two hours before fixation in 2% Neutral
233 buffered formalin (Sigma) for 10 minutes. For HIV-$1_{\Delta EnvNL4-3-GFP-Vpr}$ (VSV-G) and HIV-1_{IN-}
234 $_{EGFP}$ (VSV-G) infections, U2OS or HeLa cells (0.2 10^5) were seeded (in a well of 8 wells
235 chamber slides (BD)) and transfected at 10 picomol with siSUGT1 or siCo. siRNAs using
236 RNAi max (Promega). Cells were then infected with 200 ng p24 of HIV-$1_{\Delta EnvNL4-3-GFP-Vpr}$
237 (VSV-G) at 48 hours post-silencing for 4 hours before 2 % neutral buffered formalin (Sigma)
238 fixation for 10 minutes. For HIV-$1_{IN-EGFP}$ (VSV-G) infections, U2OS or HeLa cells at 48
239 hours post- siRNA silencing were infected with 500 ng p24 of the virus with the addition of
240 polybrene (10 µg/ml) during the different times of infection before fixation with 2 % neutral
241 buffered formalin (Sigma) or with cold methanol for EB1 staining. When U2OS cells were
242 analysed by live imaging microscopy, they were plated in ibidi 8 well chamber slides
243 (ibiTreat) before siRNA transfection.
244 For the lentiviral vectors pLKO.1, pLKO.1-shSUGT1-3'UTR-1
245 (5'CCGGGCTCTCATCGTATTGTGTATACTCGAGTATACACAATACGATGAGAGC

TTTTT3') and pLKO.1-shSUGT1-3'UTR-2: (5'CCGGATTGTGTATATTCACCTAATGCT CGAGCATTAGGTGAATATACACAATTTTTTG3'), pRLL-EF1-PGK-GFP, PRLL-EF1-SUGT1-PGK-GFP were produced by transfecting 3 10^6 HEK293T cells with 1 µg pDM2-VSV-G, 2.5 µg pΔ8.91 packaging and 2 µg the lentiviral vector using JetPRIME transfectant (Polyplus). Supernatants were harvest at 72 hours post-transfection and quantified for p24 content by ELISA. MDM (1 10^5) were transduced simultaneously using 1.5 µg p24 of each pLKO.1-shSUGT1 and/or 2µg PRLL-EF1-SUGT1-PGK-GFP (pSUGT1) and/or with the equal amounts of control empty lentiviral vectors, with the addition of polybrene during transduction (10 µg/ml), for 6 hours at 37°C and then kept for 72 hours before analysis by WB or infections. HEK293T cells (10^6) were infected with 20 ng CAp24 HIV-$1_{\Delta EnvNL4-3-Luc}$ (VSV-G) after 48 hours of transfection with pCMV-SPORT6-SUGT1 (for SUGT1 bulk transfection) or pEGFP-N1-GFP control plasmid (for SUGT1 bulk transfection) or after 72 hours of pRLL-EF1-SUGT1-PGK-GFP transfection and 24 hours after GFP-based flow cytometry sorting.

Quantitative PCR

The quantification of the HIV-1 early reverse transcripts (ERT), late Reverse Transcripts (LRTs), 2-LTRs circles and integrated proviruses were performed as previously described (10); (14). DNA was extracted with the DNeasy Tissue Kit (Qiagen) at 6- and 24 hour post-infection (h.p.i.) for ERT detection, 24 and 72 h.p.i. for LRT and 2-LTRs detections, at 48 and 72 h.p.i. for integrated proviruses, respectively, in PBLs and MDMs. The qPCR analysis was carried on an ABI prism 7000 Sequence Detection System. The amounts of HIV-1 cDNA copies were normalized to the endogenous reference gene albumin. Standard curve were generated by serial dilutions of a commercial human genomic DNA (Roche).

Immunofluorescence, confocal microscopy, SIM and live imaging

Brain autopsies of frontal cortex from three uninfected individuals and three HIV-1 infected persons were obtained in accordance with the Italian and EU legislations, after approval by the Institutional Review Board of the National Institute for Infectious diseases Lazzaro Spallanzani. Autopsies were deparaffinized, rehydrated and subjected to high-temperature antigen retrieval (96°C for 30 minutes) in 10 mM sodium citrate buffer, pH 6. After one hour blocking in 0.1% BSA in PBS, autopsies were incubated at 4°C for overnight with the primary antibodies anti-SUGT1 (Abcam, #ab30931) and anti-CAp24 (Abcam, #ab9044) diluted at 1/20 in 0.1% BSA in PBS. After three washings in PBS, the secondary antibodies anti-rabbit and anti-mouse IgG conjugated to Alexa-fluor 488 (#A11001, #A11034) and 647 fluorochromes (#A21245) from Invitrogen, respectively, and/or the recombinant anti-Iba1 conjugated to Alexa Fluor 568 with Hoechst 33342 (Invitrogen, #1874027) for nuclei were added at 1/500 dilution for two hours at room temperature. Immunostained autopsies were then mounted onto glass slides with Fluoromount G (Southern Biotech). At least 5 mosaic autopsy fields (115.33x115.33 µm each) were acquired by confocal microscopy (SP8, Leica) using a 63X objective. SP8 confocal microscope is equipped with two PMT and two high sensitivity hybrid detectors. Z series optical sections for autopsies were at 0.8 µm steps. HEK293T, HeLa and U2OS cells were rinsed with PBS, fixed with 2% neutral buffered formalin (Sigma) for 10 minutes, permeabilized for 15 minutes with 0.3% Triton-X100 in PBS, washed twice in PBS and then blocked for one hour at room temperature in 10% FBS in PBS prior to the incubation with the primary antibodies in 10% FBS in PBS for 2 hours at room temperature. For anti-EB1 staining, the fixation was performed with cold methanol on ice for 2 minutes. After three washes in PBS, the secondary antibodies conjugated with Alexa-Fluor 488 (#A11001; #A11034), 546 (#A20189; #A11035) or 647 (#A21245) (1/500, Invitrogen) supplemented with Hoechst 33342 (Invitrogen, #1874027) for nuclei staining in

296 10% FBS in PBS were added to the cells for 30 minutes at room temperature. After three PBS
297 washings, cells were then mounted with Fluoromount G (Southern Biotech), except for SIM
298 visualization U2OS cells were mounted with ProLong antifade mountant (Thermofisher
299 Scientific) and incubated for 5 hours at 30°C prior analysis. The antibodies used for cells
300 immunostaining were: anti-SUGT1 (BD Transduction Laboratories, #61204) for HEK293T
301 cells and PBLs, anti-SUGT1 (Abcam, #ab30931) for U2OS cells, anti-HA (Biolegend,
302 #90513), anti-phospho-H2AX (Ser139) (Millipore,#05-636), anti-α-tubulin (Sigma, #T9026),
303 anti-α-tubulin (Curie Institute, A-R-H#02 2017), anti-acetylated α-tubulin on lysine 40
304 (Sigma, #T6793), anti-EB1 (BD transduction laboratories, #610535), anti-HIV-1-CAp24
305 (Abcam, #ab9044) and anti-Iba1-Alexa-Fluor 568 (Abcam, #ab221003). Cells were mainly
306 imaged by confocal microscopy (SP8, Leica) using hybrid detectors (pinhole airy: 0.6; pixel
307 size: 180 nm) at optimal optical sectioning (OOS) of 0.2 µm. For acetylated □-tubulin and
308 EB1 comets, the OOS was 0.11 µm. Fluorescence intensity related to SUGT1 and
309 microtubule expressions were quantified by Image J software in the best focal plan for the
310 total cell expression for at least 100 cells. The number of acetylated α-tubulin signals and the
311 length of EB1 comets at the cell cortex were analyzed on maximum intensity of z projection
312 images obtained by Image J software. Briefly, scan lines were drawn at the levels of cell
313 cortex, EB1 comets. Then, the number of fluorescence intensity peaks for acetylated α-
314 tubulin and the length of EB1 comets were quantified using Image J software. The viral
315 particles of HIV-$1_{\Delta EnvNL4-3-GFP-Vpr}$ (VSV-G) immunofluorescence were performed as
316 previously described (15) and then were visualized by confocal microscopy (SP8, Leica)
317 using hybrid detectors (pinhole airy: 0.6; pixel size: 180 nm) and parameters adjusted for
318 deconvolution by Huygens software (Scientific Volume). For U2OS cells, acquisitions were
319 performed in 3D SIM mode, with a N-SIM structured illumination Nikon microscope before
320 image reconstruction using the NIS Elements software. The system is equipped with an APO

321 TIRF 100x 1.49NA oil immersion, a laser illumination (488nm, 200mW and 561nm,
322 100mW) and an EMCCD DU-897 Andor camera. Images were acquired with the following
323 protocol: a Z stack (0.12 µm step) was acquired. Images were then reconstructed using Nikon
324 elements software. The lateral resolution of SIM microscopy is about 32 nm. The distances
325 between two different fluorochrome-labeled proteins for SIM microscopy images were
326 calculated on one Z-stack and using "Spot function> colocalize spot" functions of Imaris 5.7
327 software (Bitplane AG) on the cropped subcellular area where GFP-labeled HIV-1 particles
328 were detected or not (HIV-1 GFP^+ or HIV-1-GFP^-). Briefly, this function determines the mass
329 center of each fluorescent molecule on the raw SIM images and determines the event number
330 of two colocalized molecules in predefined distance segment. Fluorescence from at least 300
331 molecules were quantified and the frequency of the events was determined by dividing the
332 events number in each distance segment by the total event numbers of the analyzed area in the
333 cytoplasm. For U2OS cells, images were also acquired with a high precision wide-field
334 Eclipse NiU Upright Microscope (Nikon) equipped for image deconvolution. Acquisition was
335 performed using a 100× Plan Apo VC 1.4 oil objective and a highly sensitive cooled
336 interlined charge-coupled device (CCD) camera (Roper CoolSnap HQ2). Acquired images
337 were denoised using NdSafir software before deconvolution. All microscopy images with
338 saturated signals were excluded. The colocalization threshold Mander's correlation coefficient
339 and the fluorescence spectrum overlap for colocalization were determined for different
340 fluorochrome-labeled proteins using Image J software, in the cropped subcellular area where
341 GFP-Vpr-labeled HIV-1 was detected in the merged SIM images. The colocalization
342 threshold Mander's correlation coefficient (with values varying from 0 to 1) is used to
343 quantify the co-localization or the co-occurrence proportion of two fluorescent probes in the
344 same pixels of the region of interest or structure (16). The threshold M1 (tM1) was used to
345 quantify the occurrence of green channel signals (HIV-$1_{IN\text{-}EGFP}$) in the pixels of the detected

red channel signals (α-tubulin). For live imaging, U2OS cells depleted for SUGT1 (siSUGT1) and control cells (siCo.) (0.5 10^5) plated in ibidi 8 well chamber slides (ibiTreat) were infected with HIV-$1_{IN\text{-}EGFP}$ (VSV-G) (250 ng CAp24) in the presence of polybrene (10 µg/ml) and Hoechst 33342 (1 µg/ml) (Invitrogen) and imaged simultaneously at 1 h.p.i. using a confocal spinning disk (CSU-X1M1; Yokogawa) microscope (DMI6000; Leica) equipped with a CoolSnap HQ2 camera (Photometrics) in heating chamber at 37°C with 5% CO2 for further 3 hours. Three field positions of each condition (siCo or siSUGT1) were imaged using a 63x oil lens (1.4 NA) every 20 min and with at least 40 series of Z stacks. The best focal plan images of the nucleus were then analyzed with Icy software for the mounting of the video and for quantification of infected cells with HIV-$1_{IN\text{-}EGFP}$ RTCs/PICs in the nucleus or those with only cytoplasmic viral events.

Western blots and immunoprecipitations

Cells were lysed in NEHN lysis buffer (20 mM Hepes pH 7.5, 300 mM NaCl, 0,5% NP40, 20% glycerol, 1mM EDTA) provided with protease and phosphatase cocktails inhibitors (Roche). Protein were quantified with Protein assay kit (Biorad) and 30 to 50 µg of cell extracts were diluted in the Laemmli buffer (Biorad), boiled for 5 min at 95 °C. Proteins were then loaded on the Nupage 10% or 12 % Bis Tris gel (Life Technologies) for electrophoresis separation and blotted on the PVDF (0.45 µm) transfer membrane (Thermo Scientific). After blocking with 5% bovine serum albumin (BSA), membranes were incubated with the primary antibodies followed by the secondary horseradish peroxidase (HRP) anti-rat and anti-rabbit, anti-mouse antibodies (Southern Biotech, #6180-01; #4050-05 and #1031-05, respectively). For co-immunoprecipitation assays, the Trueblot HRP secondary antibodies used were from eBioscience (#18-8816-33; #18-8817-33). The proteins were revealed by G:Box I CHEMI developer (Syngene, Ozyme) by using Super Signal West pico (Pierce) or ECL prime (GE

healthcare). The primary antibodies used were: anti-SUGT1 (BD Transduction Laboratories, #61204), anti-HA (3F10, Roche, #11867423001), anti-GAPDH (Millipore; #MAB374), anti-CAp24 (NIH AIDS research reagents, #4250), anti-Actin (Abcam, #ab49900), anti-acetylated α-tubulin K40 (AcK40-α-tubulin) (Sigma, #T6793), anti-α-tubulin (Sigma, #T9026) and, anti-HIV-1 integrase (IN-2) (Santa-Cruz, #sc-69721) in 5% skimmed milk in TBS-1% tween. For immunoprecipitations, HEK293T cells expressing HA-IN through transfection at 48 hours post transfection or U2OS cells infected for 4 hours with HIV-1$_{\square EnvNL4-3-Luc}$ (VSV-G) were harvest and then lysed in NEHN buffer. Anti-HA (3F10; Roche, #11867423001) or anti-SUGT1 (Abcam, #ab30931) (2.5 µg) were added to the cell lysates (1 mg) for 12 hours incubation at 4°C on the wheel. Then, 30 µl of the protein G sepharose 4 fast flow beads (GE healthcare) were added for additional 4 hours incubation. Immuno-complexes immobilized on the beads were washed twice with NEHN buffer (300 mM NaCl) and third time with NEHN buffer (500 mM NaCl), resuspended in Laemmli buffer (Biorad) and boiled at 95°C for 5 minutes. Immunocomplexes were then analyzed by WB.

Statistical analysis

We used the two-tailed unpaired t-test for two group comparison and the two-way ANOVA test for the multiple comparisons (more than two groups) of the absolute values means, means of frequencies or means of fold changes ± SEM (standard error of the mean). Fold changes were calculated as the ratio of the mean value from the treated sample to the mean value of the control sample. The statistical tests were represented in the figures for n>10 sample size. When n<10, the experiments were represented as individual data points without error bars. Data were analyzed with Graphpad prism 6 software. Statistical significance was given as *p <0.05 and **p <0.01, ***p<0.001, ****p<0.0001.

Results

The SUGT1 protein promotes permissiveness to HIV-1 infection

Confocal immunofluorescence microscopy was used to evaluate SUGT1 expression at the single cell level in brain frontal cortex sections from HIV-1 infected and uninfected persons. Interestingly, infected cells expressed higher levels of SUGT1, as compared to uninfected cells within the same HIV-1 patient brain section or cells in the brain sections of uninfected controls (Fig. 1a-d). These cells also expressed the ionized calcium-binding adaptor protein-1 (Iba1, Supplementary Fig. S1a), indicating that SUGT1 is increased in macrophages/microglia of HIV-1 patient brain sections. Furthermore, SUGT1 expression was increased in activated T cells, which are susceptible to HIV-1 infection as compared to resting primary T lymphocytes, which resist HIV-1 infection (Fig. 1e and Supplementary Fig. S1b). The expression of SUGT1 also strongly increased in primary monocyte-derived macrophages (MDMs), which are permissive for HIV-1, compared with monocytes, which are refractory to HIV-1 infection (Fig. 1f and Supplementary Fig. S1c), indicating that SUGT1 expression increases in permissive cells. We then analyzed the impact of SUGT1 depletion on HIV-1 replication. SUGT1 was silenced using a smart pool of small interfering RNAs (siSUGT1) in MDMs (Fig. 1g). SUGT1-depleted MDMs were infected with R5-tropic HIV-1_{AD8}, and viral replication was determined by quantifying CAp24 release. SUGT1 depletion strongly suppressed HIV-1 replication without affecting cell viability (Fig. 1j,k and Supplementary Fig. S1d). These results were confirmed in activated primary blood T-lymphocytes (PBLs) (Fig. 1h,m and Supplementary Fig. S1e,f) and in cervical epithelial (HeLa) cells engineered to express CD4/CXCR4 and a Tat-inducible β-galactosidase (β-Gal) (Fig. 1i,n and Supplementary Fig. S1g). These results were corroborated using a different SUGT1 siRNA (siSUGT1-1) (Supplementary Fig. S1h-j) and revealed no effects on CD4 and CXCR4 expression levels nor on cell viability (Supplementary Fig. S1k,l). In addition, long term

421 analysis of CAp24 release from MDMs or PBLs that were infected, respectively, with R5-
422 tropic HIV-1_{AD8} or X4-tropic HIV-1_{NL4-3} (Fig. 1o,p and Supplementary Fig. S1m-p) showed
423 that SUGT1 depletion abolished HIV-1 replication and further indicated that SUGT1 is a
424 permissive factor for HIV-1 infection.
425
426 **The early pre-integrative steps of HIV-1 life cycle are controlled by SUGT1**
427 To identify the viral replication steps that are controlled by SUGT1, MDMs and PBLs were
428 silenced for SUGT1 and infected with *luciferase* (Luc)-expressing HIV-$1_{\Delta EnvNL4-3-Luc}$ (HIV-
429 1_{VSV-G}), which is defective in the HIV-1 envelope and pseudotyped with a VSV-G envelope
430 (which allows the virus to enter cells by endocytosis). SUGT1 depletion strongly reduced the
431 infectivity of HIV-$1_{\Delta EnvNL4-3-Luc}$ (VSV-G) in MDMs (Fig. 2a,b) and PBLs (Fig. 2c,d),
432 implying that SUGT1 modulates post-entry steps. In MDMs (Fig. 2e) and PBLs (Fig. 2f)
433 whose SUGT1 had been depleted by a pool of two short hairpin RNAs (shSUGT1), the
434 expression of SUGT1 cDNA resistant to shSUGT1 restored the infectivity of HIV-$1_{\Delta EnvNL4-3-}$
435 $_{Luc}$ (VSV-G) (Fig. 2g (for MDMs) and Fig. 2h (for PBLs)). Consistently, the exogenous
436 SUGT1 overexpression in HEK293T cells significantly enhanced the infectivity of HEK293T
437 cells with HIV-$1_{\Delta EnvNL4-3-Luc}$ (VSV-G) (Supplementary Fig. S2a-d), demonstrating the specific
438 effect of SUGT1 in promoting HIV-1 infection.
439 MDMs and PBLs were then depleted for SUGT1, infected with the same virus and analyzed
440 by quantitative real time PCR (qPCR) for early reverse transcripts (at 24 and 6 hours post-
441 infection (h.p.i.) of MDMs and PBLs, respectively), late reverse transcripts and 2-LTR circles
442 (at 72 and 24 h.p.i, respectively), as well as integrated proviruses (at 72 and 48 h.p.i,
443 respectively). No significant difference in the formation of HIV-1 early reverse transcripts
444 was observed in SUGT1-depleted cells (Fig. 2i,j). A mild decrease of the late reverse
445 transcripts was observed in SUGT1-depleted MDMs (Fig. 2k) or PBLs (Fig. 2l) (as compared

with control cells). More importantly, SUGT1 depletion strongly inhibited the formation of 2-LTR circles, a surrogate marker of nuclear viral import, in HIV-1 infected MDMs (Fig. 2m) and PBLs (Fig. 2n). Consequently, the integrated proviruses (detected by the Alu-nested qPCR) were decreased after SUGT1 depletion (Fig. 2o,p). Similar results were obtained when SUGT1-depleted MDMs were infected with R5-tropic HIV-1_{AD8} (Supplementary Fig. S2e-h). The nuclear import (as evaluated by 2-LTR circles qPCR) of a HIV-1 mutant that is defective for integration (HIV-$1_{\Delta EnvNL4-3-IND64E}$ (VSV-G)) was also abrogated by the depletion of SUGT1 (Fig. 2q). Considering that mutant HIV-1_{IND64E} translocates efficiently to the nucleus (17), this result implies that SUGT1 regulates HIV-1 pre-integrative phases. To further characterize this process, we infected SUGT1-depleted HEK293T cells with HIV-$1_{CMVGFP-I-SCEI}$ (VSV-G), which encodes GFP as reporter gene and has been engineered by inserting, into the viral DNA, the yeast ISCEI endonuclease cleavage site that is cut when its cognate enzyme is introduced into human cells (11). In this system, the depletion of SUGT1 in HEK293T cells strongly inhibited HIV-1 infection, as revealed by the reduction of the percentage of cells that express immunofluorescent γH2AX-associated foci as well as the expression of virus-encoded GFP (Fig. 2r,s). The lack of GFP detection in SUGT1-depleted cells indicates the absence of 2-LTR's circles forms (which can express the GFP reporter gene) and further suggests that SUGT1 governs the nuclear translocation of HIV-1. Altogether, these data imply that SUGT1 expression dictates HIV-1 permissiveness by promoting HIV-1 reverse transcription and mainly nuclear import.

SUGT1 is associated with microtubules bearing HIV-1

Considering the role of SUGT1 in the stabilization and attachment of proteins to the microtubule network (4), we investigated the presence of SUGT1 on microtubules bearing HIV-1. U2OS cells were infected with a VSV-G-pseudotyped HIV-$1_{\Delta EnvNL4-3,}$ which

471 incorporates GFP-Vpr (HIV-$1_{\Delta EnvNL4-3-GFP-Vpr}$ (VSV-G)) (15), and the subcellular localization
472 of SUGT1, GFP-labeled viral complexes and microtubules was analyzed by super-resolution
473 structured illumination microscopy (SIM) and wide-field high precision microscopy at 4
474 hours post-infection. As expected, at this time point, GFP-labeled viral complexes colocalized
475 with cytoplasmic filaments (Fig. 3aI) and aggregated at microtubule-organizing centers
476 (MTOC) (Supplementary Fig. S3a). Importantly, endogenous SUGT1 molecules were located
477 in close proximity to the microtubule-associated viral complexes (Fig. 3aII). SUGT1, viral
478 complexes, and microtubules often formed ternary structures (Fig. 3aII1-4). Fluorescence
479 overlap spectrum analysis confirmed these results, indicating that the three components
480 (SUGT1, GFP and microtubules) were located within a distance of <0.8 μm (Fig. 3aII1-4). A
481 high colocalization Mander's coefficient (~1) confirmed the tight association of SUGT1 with
482 microtubules that are used by HIV-1 for trafficking in host cells (Supplementary Fig. S3b,c).
483
484 Since HIV-1 integrase (IN) translocates to the nucleus to catalyze the integration of viral
485 cDNA into the human genome, we monitored the subcellular localization of HA-tagged
486 integrase (HA-IN) in SUGT1-depleted U2OS cells. Interestingly, we observed that the
487 silencing of SUGT1 (Fig. 3b) induced a diffused localization of IN in the cytoplasm and the
488 nucleus compared with control cells that had exclusive nuclear localization (Fig. 3c,d),
489 indicating that SUGT1 contributes to the nuclear accumulation of IN. In agreement with a
490 previous report showing that efficient nuclear translocation prevents cytoplasmic degradation
491 of HIV-1 IN (18), protein levels of HA-IN decreased in SUGT1-depleted cells (Fig. 3b).
492 However, no interactions between endogenous SUGT1 and HA-IN were detected by co-
493 immunoprecipitation in HEK293 T cells (Fig. 3e), suggesting that SUGT1 may act on HIV-1
494 nuclear translocation without interacting with viral proteins. Altogether, these data indicate
495 that SUGT1 is associated with microtubules bearing HIV-1.

SUGT1 regulates the organization and the stability of the cortical microtubule plus-ends

To understand the mechanism by which SUGT1 contributes to HIV-1 nuclear import, we investigated the effect of SUGT1 on the structural organization of microtubules. Although SUGT1 knockdown did not modify tubulin expression, nor disrupt the global architecture or the density of the microtubule network (Fig. 4a,b and Supplementary Fig. S4a,b), confocal microscopy revealed a significant alteration of the microtubule plus-ends (+MTs) organization at the level of the cell cortex (Fig. 4a,c and Supplementary Fig. S4a). SUGT1-depleted U2OS cells exhibited +MTs that were dissociated and distributed perpendicularly to the cell cortex, while in control cells, the +MTs were clustered and curved in parallel to the cell cortex. Even though the total expression of stable microtubules (AcK40 α-tubulin) was not affected by the SUGT1 knockdown (Supplementary Fig. S4b), the acetylation of +MTs at the cell cortex significantly decreased in U2OS and HeLa cells (Fig. 4d-f and Supplementary Fig. S4c-f). These data indicate that the cortical +MTs, which are the first contact points of HIV-1 with the microtubule network after viral entry, are unstable in SUGT1-depleted cells and thus may not efficiently support the cytoplasmic trafficking of the virus. To confirm this hypothesis, we analyzed whether SUGT1 depletion would affect the organization of the plus-end tracking protein EB1, which promotes the cytoplasmic trafficking of HIV-1 on microtubules (1). Considering that EB1 molecules bind to +MTs and form EB1 comets, whose elongation is associated with an increased growth rate and a decreased stability (19-22), the impact of SUGT1 silencing on the length of EB1 comets was determined. A significant increase in the length of EB1 comets was observed in SUGT1-depleted HeLa and U2OS cells, compared with control cells (Fig. 4g-i and Supplementary Fig. S4g-j), suggesting that in SUGT1-depleted cells, +MTs are less stable and highly dynamic, and thus would not sustain the trafficking of HIV-1 viral particles after viral entry. Taken together, our data

521 reveal that SUGT1 controls the architecture and the stability of +MTs, which are required for
522 the attachment and efficient trafficking of HIV-1 on the microtubule network.
523

524 **SUGT1 is essential for the association of HIV-1 with stable microtubules and its**
525 **translocation to the host cell nucleus**

526 Co-immunoprecipitation assays revealed an interaction between SUGT1 and stable
527 microtubules (Fig. 5a). This interaction was strongly enhanced after 4 hours of infection of
528 U2OS cells with HIV-$1_{\Delta EnvNL4\text{-}3\text{-}Luc}$ (VSV-G), further demonstrating that SUGT1 is associated
529 with the microtubules that are used by HIV-1 for trafficking (Fig. 5a). Using HIV-$1_{IN\text{-}EGFP}$
530 virus pseudotyped by VSV-G envelope that contains enhanced GFP labeled IN (12, 23), we
531 showed that in SUGT1-depleted U2OS cells, and in contrast to control cells (Fig. 5b), HIV-
532 $1_{IN\text{-}EGFP}^{+}$ viral complexes did not aggregate at the MTOC and displayed a diffuse distribution
533 in the cytoplasm (Fig. 5d). Accordingly, the colocalization of HIV-$1_{IN\text{-}EGFP}^{+}$ complexes with
534 microtubules significantly decreased in SUGT1-depleted cells (Fig. 5c), suggesting that, in
535 the absence of SUGT1, a defect in the migration to the perinuclear area is associated with a
536 defect in the association of the virus with microtubules. In agreement with the results obtained
537 with HIV-1 IN expressed as a single protein (Fig. 3b), the mean fluorescence intensity of
538 HIV-$1_{IN\text{-}EGFP}^{+}$ complexes detected after 4 hours of infection of SUGT1-depleted cells was
539 significantly decreased, as compared with control cells (Supplementary Fig. S5a), indicating
540 that the failed nuclear translocation of HIV-1 induces its rapid cytoplasmic degradation.
541 Moreover, SUGT1 depletion decreased the percentage of cells with HIV-$1_{IN\text{-}EGFP}$ nuclear
542 events at 4 and 6 h.p.i. and increased the percentage of cells showing only cytoplasmic viral
543 events (Fig. 5e). Consistent with these results, live imaging microscopy showed nuclear
544 translocation of HIV-$1_{IN\text{-}EGFP}^{+}$ viral complexes in control U2OS cells (Movie 1), while in the
545 SUGT1-depleted cells, viral complexes did not translocate to the host cell nucleus (Movie 2),

leading to a decrease of HIV-1 nuclear events (Supplementary Fig. S5b). Interestingly, a significant elongation of EB1 comets was detected in SUGT1-depleted HeLa cells infected with HIV-$1_{IN\text{-}EGFP}$ (VSV-G) (Fig. 5f,g) or HIV-$1_{\Delta EnvNL4\text{-}3\text{-}Luc}$ (VSV-G) (Supplementary Fig. S5c) for 6 hours, as compared with control cells. Accordingly, the nuclear accumulation of HIV-$1_{IN\text{-}EGFP}^{+}$ viral complexes was significantly decreased in SUGT1-depleted cells (Fig. 5h). Altogether, these results demonstrate that SUGT1 promotes HIV-1 nuclear import by increasing its association with microtubules and its cytoplasmic trafficking to reach the host nucleus.

SUGT1 depletion abolished permissiveness to HIV-1 primary isolates and ART-resistant viral mutant

In order to evaluate the potential of SUGT1 inactivation for HIV-1 therapy, we determined the impact of SUGT1 depletion on the permissiveness of MDMs to infection with HIV-1 primary isolates (HIV-1_{BXO8}, HIV-1_{132W} and HIV-1_{DH12}) and to HIV-1 clone (HIV-$1_{140/148}$), a double mutant virus that is resistant to raltegravir antiretroviral treatment (ART) (13). Interestingly, SUGT1 depletion strongly inhibited the formation of 2-LTR circles (Fig. 6a-d) and CAp24 release (Fig. 6e-g) from MDMs that were infected with CCR5 (R5) tropic (HIV-1_{BXO8} and HIV-1_{132W}) or CCR5/CXCR4 (R5X4) dual tropic (HIV-1_{DH12}) HIV-1 primary isolates (Fig. 6a-e). In addition, the depletion of SUGT1 drastically impaired viral integration (Fig. 6h) and CAp24 release (Fig. 6i) from MDMs that were infected with an HIV-1 double mutant G140S-Q148H in integrase polypeptide (HIV-$1_{140/148}$) that is resistant to the integrase inhibitor raltegravir. Altogether, these results highlight the potential for SUGT1 as a cellular target to inhibit viral replication and overcome viral resistance to ART.

Discussion

In the present study, we demonstrate that SUGT1 is a host factor that determines lymphocyte and macrophage susceptibility to HIV-1 infection and replication via an effect on the post-entry replication steps. SUGT1 stabilizes the +MTs, thereby promoting the association of HIV-1 with stable microtubules, allowing their efficient trafficking to the nuclear pores, and viral import into the nucleus and subsequent integration into the host genome. In contrast to the previously described microtubule-associated proteins (such as EB1 and Kif4 (1-3, 24)), which increase microtubule stability (by enhancing AcK40 α-tubulin) following infection, SUGT1 contributes to maintain the stability of microtubules mainly at the level of the plus-end TIPs, by inhibiting their dynamic and preserving their acetylation. The fact that we showed that SUGT1 expression is upregulated in the HIV-1 permissive activated T cells and macrophages with respect to their cognate resting lymphocytes and monocytes refractory to HIV-1 infection, does not exclude the possible contribution of synergetic pathways involved during differentiation and activation in the stabilization of the microtubules and enhancing the susceptibility to HIV-1. A recent report demonstrated that the rapid proteasome-mediated degradation of the viral cores in the cytoplasm is detected when their uncoating fails to occur progressively up to their trafficking to the nuclear pores (25). Consistent with this report, the intensity of the fluorescent viral complexes, which were mainly accumulated in the cytoplasm of host cells, was significantly decreased in SUGT1-depleted cells, as compared with control cells, suggesting their degradation by proteasomes due to lack of efficient trafficking to the nuclear pores. Similarly, HIV-1 IN was shown to be stabilized on the MTOC, prior to its nuclear translocation, through direct interaction with microtubule–associated proteins (such as the centrosomal protein STU2P (yeast homolog of XMAP215) and the dynein light chain protein DYN2P) (26, 27) and its failure to be recruited to the nucleus leads to its rapid degradation by proteasomes in the cytoplasm of host cells (18). Future studies will explore the

595 potential role of SUGT1 in the trafficking of other viruses that employ the microtubule
596 network, such as Hepatitis C virus, Dengue virus or African Swine Fever virus. Finally, our
597 results demonstrate that SUGT1 should be considered as a target in novel therapeutic
598 strategies to inhibit infection with HIV-1 strains that are resistant to raltegravir antiretroviral
599 treatment (ART).
600

Acknowledgements

We acknowledge Dr. Alessandro Donado, Yann Lecluse, Floriane Herit and Pierre Bourdoncle (IMAG'IC facility of Institut Cochin) for their technical support, and Pr. Eric Solary for the pRLL-EF1-PGK-GFP lentiviral vector plasmid. This work was supported by funds from Agence Nationale de la Recherche (ANR-10-IBHU-0001, ANR-10-LABX33 and ANR-11-IDEX-003-01), Cancéropole Ile de France, Electricité de France, Fondation Gustave Roussy, Institut National du Cancer (INCA 9414), NATIXIS, SIDACTION and the French National Agency for Research on AIDS and viral Hepatitis (ANRSH) (to J-L.P. and F.N.).

Conflict of interest

The authors declare they have no conflicts of interest.

References

1. Sabo Y, Walsh D, Barry DS, Tinaztepe S, de Los Santos K, Goff SP, et al. HIV-1 induces the formation of stable microtubules to enhance early infection. *Cell Host Microbe*. 2013;**14**:535-546.

2. Delaney MK, Malikov V, Chai Q, Zhao G, Naghavi MH. Distinct functions of diaphanous-related formins regulate HIV-1 uncoating and transport. *Proc Natl Acad Sci U S A*. 2017;**114**:E6932-E6941.

3. Dharan A, Campbell EM. Role of Microtubules and Microtubule-Associated Proteins in HIV-1 Infection. *J Virol*. 2018;**92**:e00085-18.

4. Andersen RO, Turnbull DW, Johnson EA, Doe CQ. Sgt1 acts via an LKB1/AMPK pathway to establish cortical polarity in larval neuroblasts. *Dev Biol*. 2012;**363**:258-265.

5. Davies AE, Kaplan KB. Hsp90-Sgt1 and Skp1 target human Mis12 complexes to ensure efficient formation of kinetochore-microtubule binding sites. *J Cell Biol*. 2010;**189**:261-274.

6. Kitagawa K, Skowyra D, Elledge SJ, Harper JW, Hieter P. SGT1 encodes an essential component of the yeast kinetochore assembly pathway and a novel subunit of the SCF ubiquitin ligase complex. *Mol Cell*. 1999;**4**:21-33.

7. Liu W, Evanoff DP, Chen X, Luo Y. Urinary bladder epithelium antigen induces CD8+ T cell tolerance, activation, and autoimmune response. *J Immunol*. 2007;**178**:539-546.

8. Steensgaard P, Garre M, Muradore I, Transidico P, Nigg EA, Kitagawa K, et al. Sgt1 is required for human kinetochore assembly. *EMBO Rep*. 2004;**5**:626-631.

9. Mayor A, Martinon F, De Smedt T, Petrilli V, Tschopp J. A crucial function of SGT1 and HSP90 in inflammasome activity links mammalian and plant innate immune responses. *Nat Immunol*. 2007;**8**:497-503.

10. Allouch A, David A, Amie SM, Lahouassa H, Chartier L, Margottin-Goguet F, et al. p21-mediated RNR2 repression restricts HIV-1 replication in macrophages by inhibiting dNTP biosynthesis pathway. *Proc Natl Acad Sci U S A*. 2013;**110**:E3997-4006.

11. Di Primio C, Quercioli V, Allouch A, Gijsbers R, Christ F, Debyser Z, et al. Single-cell imaging of HIV-1 provirus (SCIP). *Proc Natl Acad Sci U S A*. 2013;**110**:5636-5641.

12. Francis AC, Di Primio C, Quercioli V, Valentini P, Boll A, Girelli G, et al. Second generation imaging of nuclear/cytoplasmic HIV-1 complexes. *AIDS Res Hum Retroviruses*. 2014;**30**:717-726.

13. Delelis O, Malet I, Na L, Tchertanov L, Calvez V, Marcelin AG, et al. The G140S mutation in HIV integrases from raltegravir-resistant patients rescues catalytic defect due to the resistance Q148H mutation. *Nucleic Acids Res*. 2009;**37**:1193-1201.

14. David A, Saez-Cirion A, Versmisse P, Malbec O, Iannascoli B, Herschke F, et al. The engagement of activating FcgammaRs inhibits primate lentivirus replication in human macrophages. *J Immunol*. 2006;**177**:6291-6300.

15. McDonald D, Vodicka MA, Lucero G, Svitkina TM, Borisy GG, Emerman M, et al. Visualization of the intracellular behavior of HIV in living cells. *J Cell Biol*. 2002;**159**:441-452.

16. Dunn KW, Kamocka MM, McDonald JH. A practical guide to evaluating colocalization in biological microscopy. *Am J Physiol Cell Physiol*. 2011;**300**:C723-742.

17. Svarovskaia ES, Barr R, Zhang X, Pais GC, Marchand C, Pommier Y, et al. Azido-containing diketo acid derivatives inhibit human immunodeficiency virus type 1 integrase in vivo and influence the frequency of deletions at two-long-terminal-repeat-circle junctions. *J Virol.* 2004;**78**:3210-3222.

18. Devroe E, Engelman A, Silver PA. Intracellular transport of human immunodeficiency virus type 1 integrase. *J Cell Sci*. 2003;**116**:4401-4408.

19. Akhmanova A, Steinmetz MO. Control of microtubule organization and dynamics: two ends in the limelight. *Nat Rev Mol Cell Biol*. 2015;**16**:711-726.

20. Bieling P, Kandels-Lewis S, Telley IA, van Dijk J, Janke C, Surrey T. CLIP-170 tracks growing microtubule ends by dynamically recognizing composite EB1/tubulin-binding sites. *J Cell Biol*. 2008;**183**:1223-1233.

21. Matov A, Applegate K, Kumar P, Thoma C, Krek W, Danuser G, et al. Analysis of microtubule dynamic instability using a plus-end growth marker. *Nat Methods*. 201;**7**:761-768.

22. Seetapun D, Castle BT, McIntyre AJ, Tran PT, Odde DJ. Estimating the microtubule GTP cap size in vivo. *Curr Biol*. 2012;**22**:1681-1687.

23. Albanese A, Arosio D, Terreni M, Cereseto A. HIV-1 pre-integration complexes selectively target decondensed chromatin in the nuclear periphery. P*LoS One*. 2008;**3**:e2413.

24. Fernandez J, Portilho DM, Danckaert A, Munier S, Becker A, Roux P, et al. Microtubule-associated proteins 1 (MAP1) promote human immunodeficiency virus type I (HIV-1) intracytoplasmic routing to the nucleus. *J Biol Chem*. 2015;**290**:4631-4646.

25. Francis AC, Melikyan GB. Single HIV-1 Imaging Reveals Progression of Infection through CA-Dependent Steps of Docking at the Nuclear Pore, Uncoating, and Nuclear Transport. *Cell Host Microbe*. 2018;**23**:536-548 e6.

26. Desfarges S, Salin B, Calmels C, Andreola ML, Parissi V, Fournier M. HIV-1 integrase trafficking in S. cerevisiae: a useful model to dissect the microtubule network involvement of viral protein nuclear import. *Yeast*. 2009;**26**:39-54.

27. de Soultrait VR, Caumont A, Durrens P, Calmels C, Parissi V, Recordon P, et al. HIV-1 integrase interacts with yeast microtubule-associated proteins. *Biochim Biophys Acta*. 2002;**1575**:40-48.

Figure legends

Figure 1. SUGT1 determines HIV-1 permissiveness in human cells.

(**a-c**) Immunofluorescence of brain autopsies from uninfected persons (n=3) (**a**) and HIV-1 infected patients (n=3) (**b**) for SUGT1, CAp24 and nucleus. (**c**) Magnification.

(**d**) Quantification of SUGT1 expression in $CAp24^+$ (n=45) or $CAp24^-$ (n=690) cells detected in brain sections. Fluorescence intensities (FI) are shown. Means ± SEM are indicated. P values were calculated using two-tailed unpaired t-test using Bonferroni correction (*p <0.1).

(**e, f**) Representative human resting/PHA-P/IL2-activated PBLs (**e**) or monocytes/macrophages (**f**) WB of endogenous SUGT1 levels are shown (n=3). SUGT1 a and b isoforms are indicated.

(**g-i**) SUGT1 depletion in human MDMs (**g**), PBLs (**h**) and $CD4^+CXCR4^+$ HeLa cells (**i**) are shown (n=3).

(**j-n**) Effect of SUGT1 depletion on viral production obtained from MDMs (**j, k**), PBLs (**l, m**) or $CD4^+CXCR4^+$ HeLa cells (n=3) (**n**) infected with HIV-1_{AD8} (**j, k**) or HIV-1_{NL4-3} (**l-n**). CAp24 release for representative donor (**j, l**) and fold changes (n=7 for MDMs, n=3 for PBLs) (**k, m**) are shown.

(**o, p**) Effect of SUGT1 depletion on viral production obtained at indicated times post-infection from MDMs (**o**) and PBLs (**p**) infected with HIV-1_{AD8} (**o**) or HIV-1_{NL4-3} (**p**). CAp24 release from representative donors is shown (n=3).

Figure 2. SUGT1 promotes early HIV-1 replication steps.

(**a-d**) HIV-1 infectivity of control or SUGT1-depleted MDMs (**a, b**) and activated PBLs (**c, d**) that were infected with HIV-$1_{\Delta EnvNL4-3-Luc}$ (VSV-G) for 72 hours. Luciferase activity from

representative donor (**a, c**) and fold changes (n=8 for MDMs and n=4 for PBLs) (**b, d**) are shown.

(**e-h**) MDMs (**e**) and PBLs (**f**) were transduced with lentiviral vectors expressing control (shCo.), a pool of two shRNAs against SUGT1 (shSUGT1) and/ or SUGT1 resistant cDNA (pSUGT1) for 72 hours prior infection with HIV-$1_{\Delta EnvNL4-3-Luc}$ (VSV-G). WB (**e,f**) and luciferase activity at 48 h.p.i. from representative donors is shown (**g,h**) (n=3).

(**i-q**) Fold changes of HIV-1 early reverse transcripts (**i, j**), late reverse transcripts (**k, l**), 2-LTRs circles (**m, n, q**) and integrated proviruses (**o, p**) were determined by qPCR in control or SUGT1-depleted macrophages (**i, k, m, o, q**) or lymphocytes (**j, l, n and p**) that were infected with HIV-$1_{\Delta EnvNL4-3-Luc}$ (VSV-G) (**i-p**) or with HIV-$1_{\Delta EnvNL4-3-IND64E}$ (VSV-G) (**q**) (n=3).

(**r, s**) Representative confocal micrographs of HIV-$_{1CMV-GFP-I-SCEI}$-infected HEK293T cells (**r**) and percentages of HIV-1 infected (GFP^+) cells with $\gamma H2AX^+$ foci (**s**) are shown. Means ± SEM are indicated (n=3). P values were calculated using two-tailed unpaired t test (**p <0.01).

Figure 3. SUGT1 is associated with microtubules trafficking HIV-1.

(**a**) Representative SIM micrograph of 4 hour HIV-$1_{\Delta EnvNL4-3-GFP-Vpr}$ (VSV-G) infected U2OS cells showing SUGT1 and α-tubulin expression (**aI**). (**aII**) is a magnification of the dashed region in (**aI**). (**aII1-4**) are the magnifications of the dashed regions in (**aII**). Fluorescence overlap spectrums of (**aII1-4**) cropped regions, are shown.

(**b**) HIV-1 IN and SUGT1 expression levels by WB in control and SUGT1-depleted U2OS cells after 48 hours siRNA transfection and expression of exogenous HIV-1 IN for 24 hours.

(**c, d**) Representative confocal micrographs of HIV-1 HA-IN expression in control and SUGT1-depleted U2OS cells (**c**) and percentages of cells showing nuclear or diffused HIV-1 IN (**d**).

(**e**) Immunoprecipitation of HA-IN in control and HA-IN-overexpressing HEK293T cells and expression of indicated proteins by WB.

WB and images are representative of three independent experiments. Means ± SEM are indicated from at least three independent experiments. P values were calculated using two-way ANOVA test (****$p<0.0001$).

Figure 4. SUGT1 stabilizes microtubule tips at the cell cortex.

(**a**) Representative confocal micrographs and magnifications showing α-tubulin and nucleus in control and SUGT1-depleted U2OS cells.

(**b**) Fluorescence intensity of α-tubulin.

(**c**) Percentages of cells with +MTs parallel or perpendicular to the cell cortex.

(**d-f**) Representative confocal micrographs of α-tubulin, AcK40 α-tubulin and nucleus in control and SUGT1-depleted U2OS cells (**d**). Magnifications (**e**). Quantification of AcK40 α-tubulin signals normalized to 100 μm of cell cortex length in cells (**f**).

(**g-i**) Representative confocal micrographs of α-tubulin, EB1 and nucleus in control and SUGT1-depleted HeLa cells (**g**). Separate fluorescence images of (**g**) are shown in Supplementary Fig. S4g,h. Magnifications (**h**). Quantification of EB1 comet length (n=559) of cells (n=60) (**i**).

Means ± SEM are indicated from at least three independent experiments. P values were calculated using two-way ANOVA test for (**c**) and two-tailed unpaired t test for (**f**) and (**i**) (****$p<0.0001$).

Figure 5. SUGT1 promotes the association between HIV-1 and microtubules.

(**a**) Co-immunoprecipitation of endogenous SUGT1 with AcK40 α-tubulin in control and HIV-$1_{\Delta EnvNL4-3-Luc}$ (VSV-G)-infected U2OS cells for 4 hours and expression of indicated proteins by WB.

(**b, d**) Representative confocal micrographs of HIV-$1_{IN-EGFP}$ virus and α-tubulin in control (**b**) and SUGT1-depleted (**d**) U2OS cells that were infected for 4 hours.

(**c**) Mander's correlation coefficient (tM1) of HIV-$1_{IN-EGFP}^{+}$ and α-tubulin in control and SUGT1-depleted U2OS cells at 4 h.p.i..

(**e**) Percentages of cells showing nuclear or cytoplasmic HIV-$1_{IN-EGFP}^{+}$ events at 4 and 6 h.p.i..

(**f**) Representative confocal micrographs of HIV-$1_{IN-EGFP}$, □□□ and nucleus in control and SUGT1-depleted HeLa cells that were infected with HIV-$1_{IN-EGFP}$ for 6 hours. Magnifications are shown.

(**g**) Lengths of EB1 comets (n=400) of cells (n=100) are determined.

(**h**) Percentages of control or SUGT1-depleted HeLa cells showing nuclear or only cytoplasmic HIV-$1_{IN-EGFP}^{+}$ events at 6 h.p.i.

Means ± SEM are indicated from at least three independent experiments. P values were calculated using two-tailed unpaired t-test for (**c**) and (**g**) and two-Way ANOVA for (**e**) and (**h**) (***$p<0.001$ and ****$p<0.0001$).

Figure 6. SUGT1 depletion impairs replication of HIV-1 primary isolates and ART mutant resistant virus.

(**a-d**) HIV-1 2-LTRs circles quantification by qPCR 72 h.p.i. with HIV-1_{BXO8} (**a, b**) and HIV-1_{132W} (**c, d**) primary isolates of control and MDMs that were silenced for SUGT1 during 72 hours. Representative donor (**a, c**) and fold changes (n=3) (**b, d**) are shown.

814 (**e-g**) HIV-1 CAp24 detected by WB in the cell supernatants (SN) of MDMs that were
815 depleted (or not) for SUGT1 and infected with HIV-1_{BXO8} (**e**), HIV-1_{132W} (**f**) and HIV-1_{DH12}
816 (**g**). Representative WB revealing CAp24, SUGT1 and Tubulin expressions are shown (n=3).
817 (**h, i**) Control and SUGT1-depleted primary human MDMs were infected with HIV-$1_{140/148}$
818 and evaluated for proviral integration and for CAp24 release at 72 h.p.i. (n=2).
819

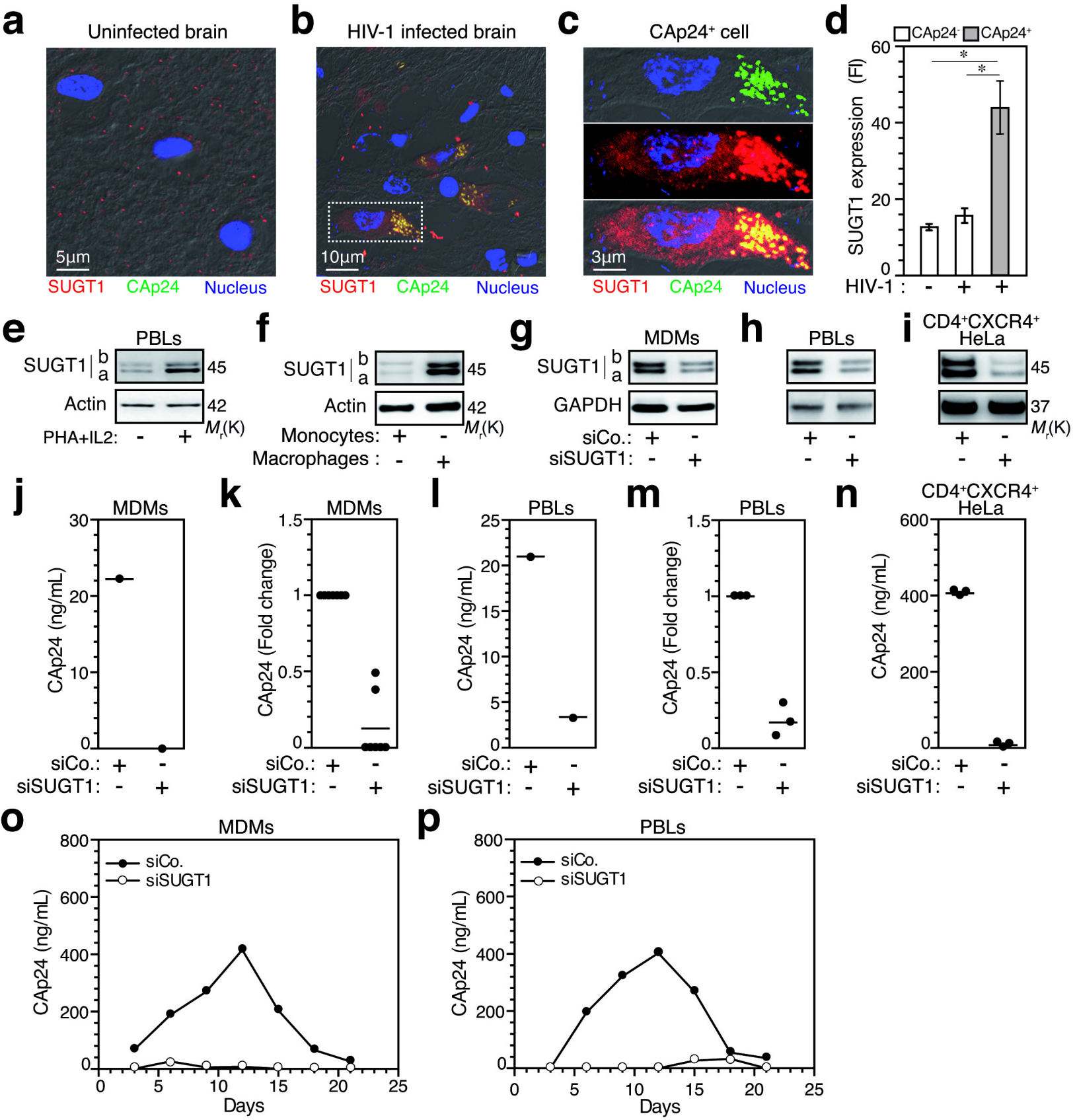

ALLOUCH CDD Revised#1

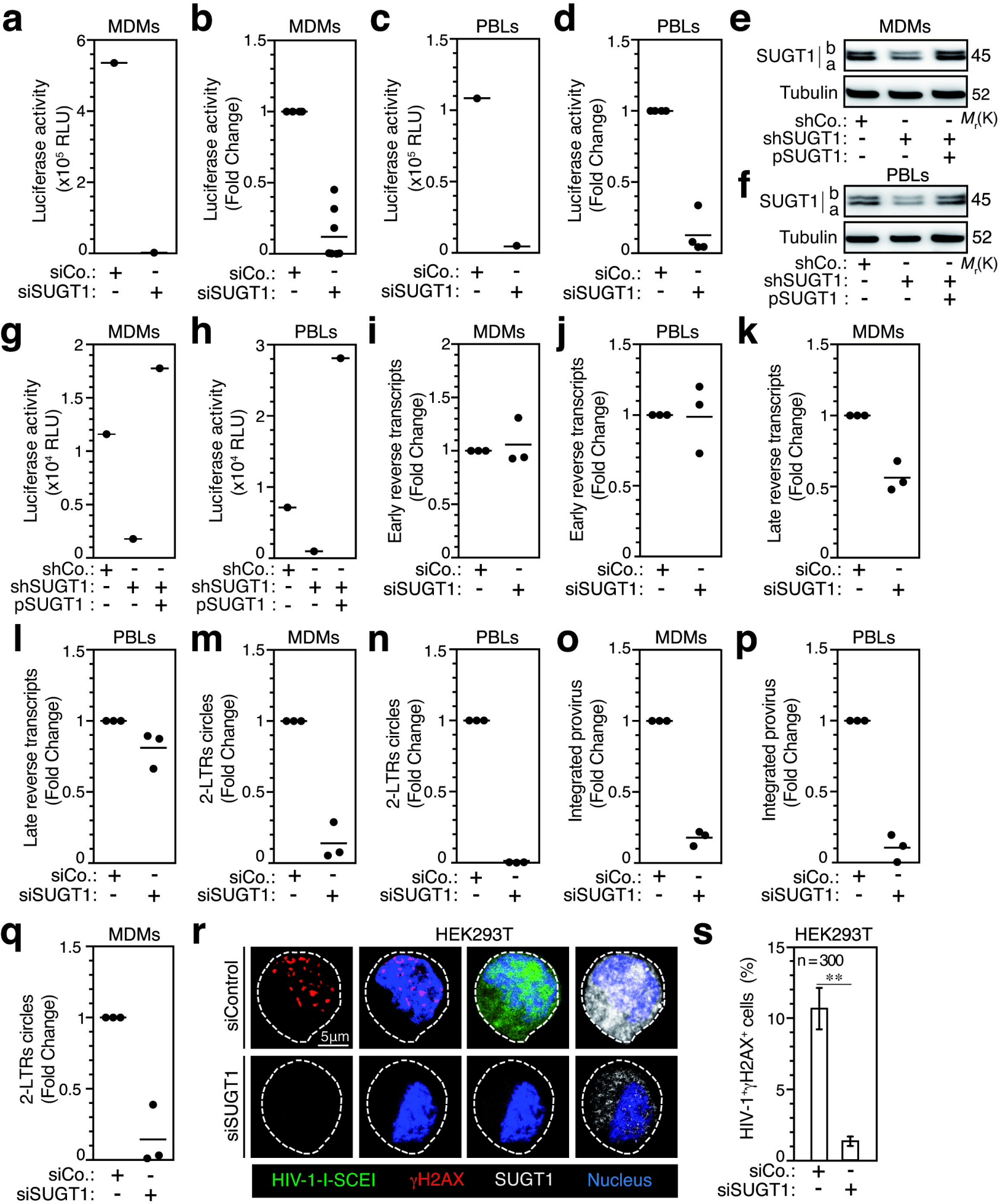

ALLOUCH CDD Revised#2

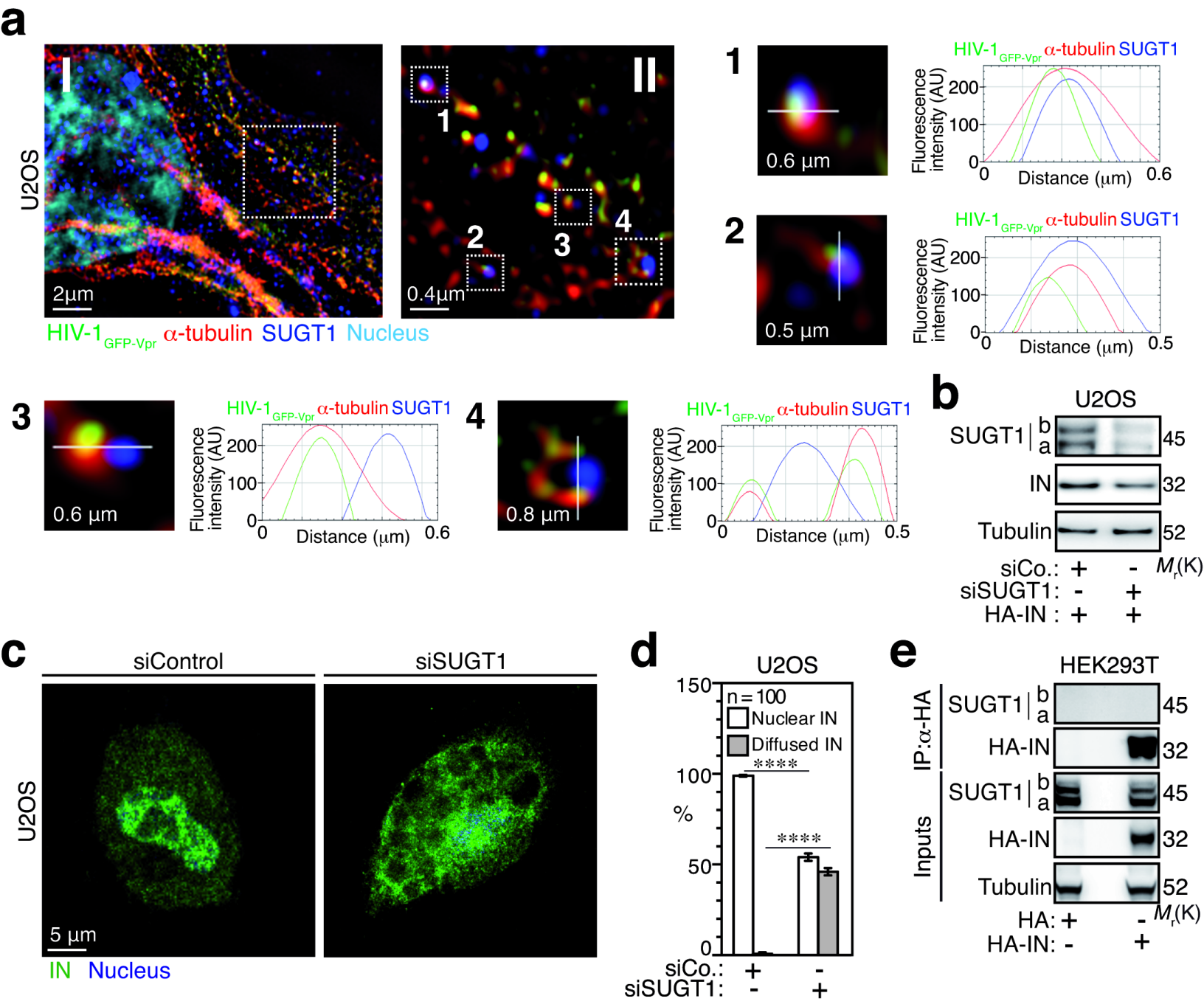

ALLOUCH CDD Corrected#3

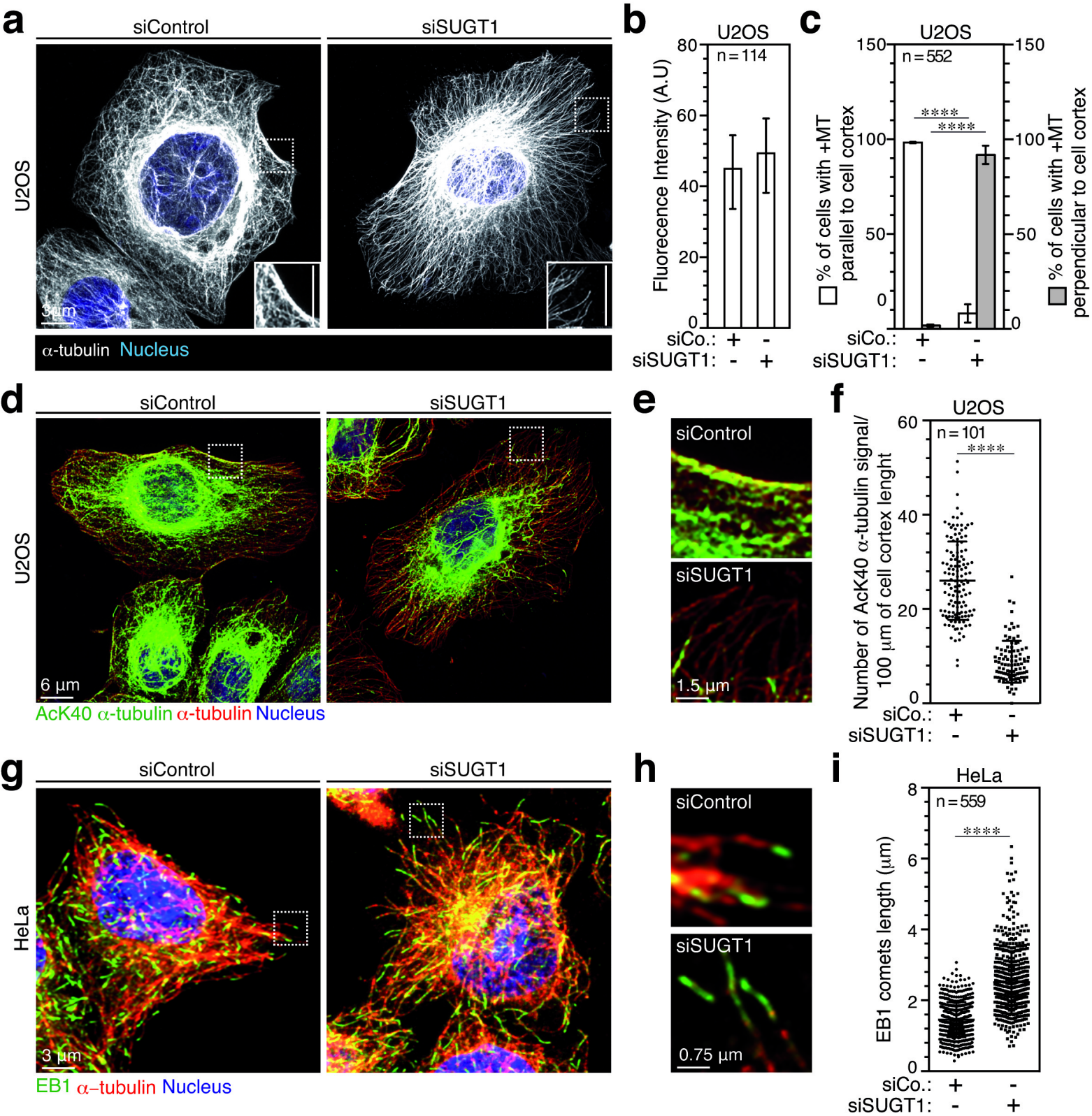

ALLOUCH CDD Revised#4

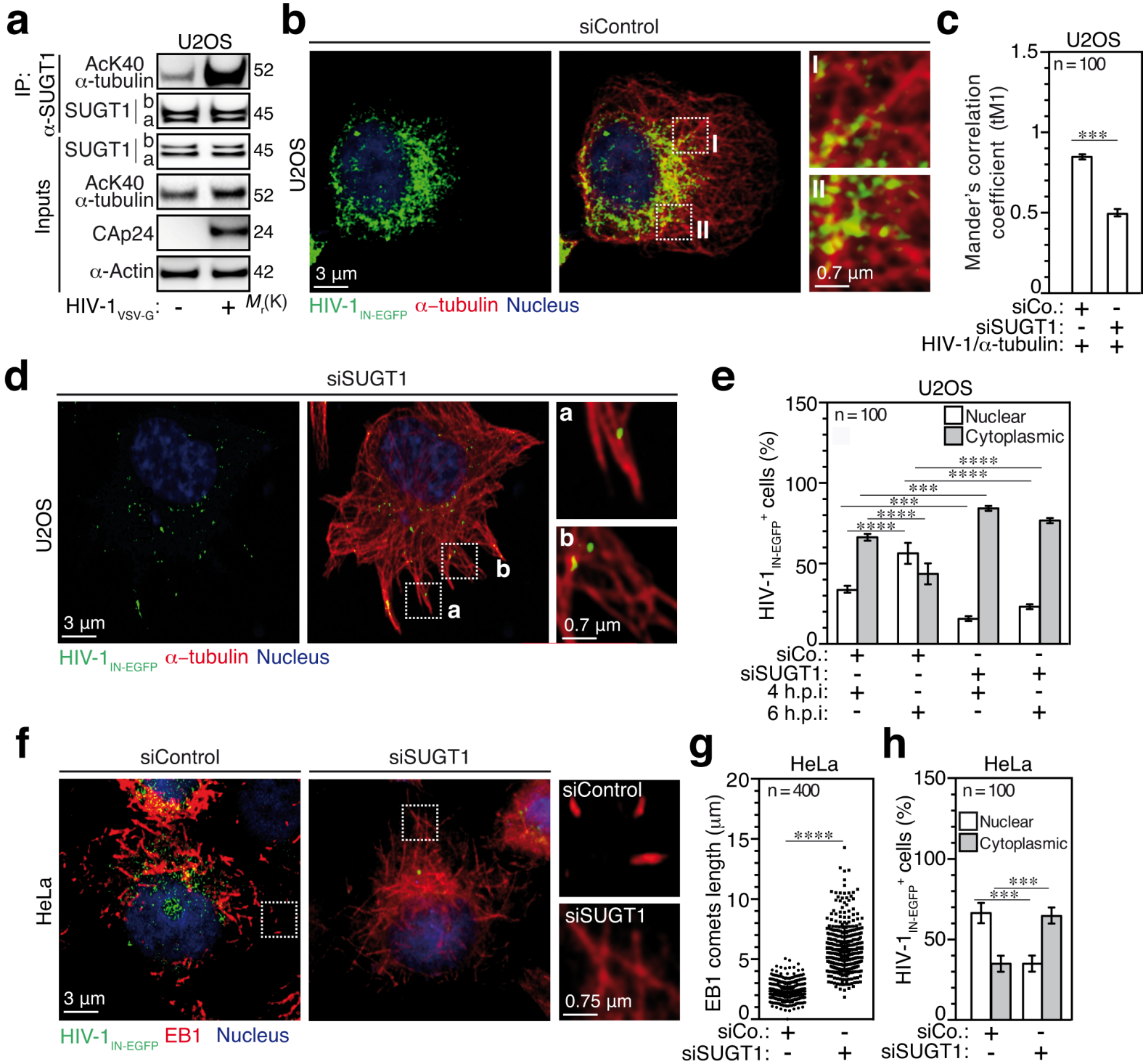

ALLOUCH CDD Corrected#5

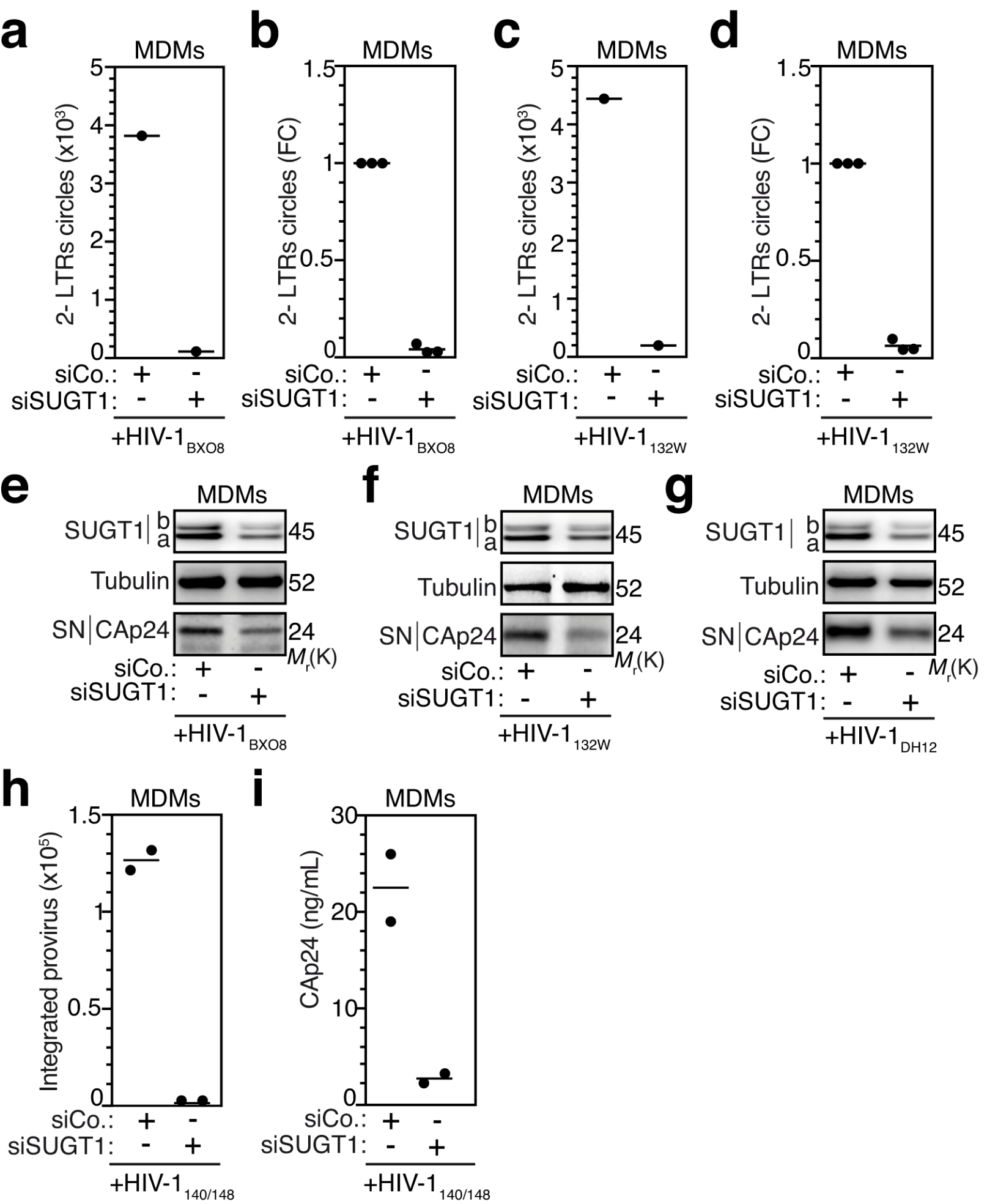

ALLOUCH CDD Corrected#6